Available online at www.sciencedirect.com

ScienceDirect

journal homepage: www.elsevier.com/locate/he

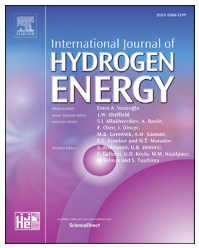

Hydrogen adsorption properties of Ag decorated TiO_2 nanomaterials

Saravanan Rajendran [a,*], *Tuan K.A. Hoang* [b], *Rabah Boukherroub* [c], *D.E. Diaz-Droguett* [d], *F. Gracia* [e,**], *M.A. Gracia-Pinilla* [f,g], *A. Akbari-Fakhrabadi* [h], *Vinod Kumar Gupta* [i,j]

[a] *Laboratory of Environmental Research on Arid Zones, LIMZA, University of Tarapacá, Chile*
[b] *University of Waterloo, 200 University Avenue West, Waterloo, ON, N2L 3G1, Canada*
[c] *Univ. Lille, CNRS, Centrale Lille, ISEN, Univ. Valenciennes, IEMN, UMR CNRS 8520, Avenue Poincaré, CS 60069, 59652, Villeneuve d'Ascq, France*
[d] *Institute of Physics, Facultad de Física, Pontificia Universidad Católica de Chile, Casilla 306, Santiago, Chile*
[e] *Department of Chemical Engineering, Biotechnology and Materials, University of Chile, Beauchef 851, 6th Floor, Santiago, Chile*
[f] *Universidad Autónoma de Nuevo León, Facultad de Ciencias Físico-Matemáticas, Av. Universidad, Cd. Universitaria, San Nicolás de los Garza, NL, Mexico*
[g] *Universidad Autónoma de Nuevo León, Centro de Investigación en Innovación y Desarrollo en Ingeniería y Tecnología, PIIT, Apodaca, NL, Mexico*
[h] *Advanced Materials Laboratory, Department of Mechanical Engineering, University of Chile, Beauchef 851, Santiago, Chile*
[i] *Department of Applied Chemistry, University of Johannesburg, Johannesburg, South Africa*
[j] *Department of Biological Sciences, King Abdulaziz University, Jeddah, 21589, Saudi Arabia*

ARTICLE INFO

Article history:
Received 20 September 2017
Received in revised form
11 December 2017
Accepted 12 December 2017
Available online 6 January 2018

Keywords:
Adsorption
Hydrogen
Nanocomposite
Kubas-type
Spillover

ABSTRACT

In this work, we present the synthesis of Ag doped TiO_2 materials. The products are characterized by powder X-ray diffraction, transmission electron microscopy, X-ray photoelectron spectroscopy, nitrogen adsorption, and hydrogen adsorption. The Ag/TiO_2 materials exhibit 3.65 times higher in hydrogen adsorption capability compared with the non-doped TiO_2 materials thank to the existence of Ti^{3+} species, which are Kubas-type hydrogen adsorption centers, and the Ag nanoparticles which provide spillover effects. We believe that this is the first time that both Kubas-type adsorption and spillover are exploited in the design of novel hydrogen storage materials.

* *Corresponding author.*
** *Corresponding author.*
E-mail addresses: saravanan3.raj@gmail.com (S. Rajendran), fgracia@ing.uchile.cl (F. Gracia).
https://doi.org/10.1016/j.ijhydene.2017.12.080

Introduction

In recent years, solid state nanomaterials such as nano-semiconductors, nanometals, nanowires, nanotubes, nanoporous, and hollow materials are exploited in the areas of energy and environment, especially for hydrogen storage owing to their high hydrogen absorption or adsorption properties with different mechanisms [1–5]. These solid state storage methods offer multiple benefits such as small size of materials, high efficiency, low weight, and low-cost compared with physical hydrogen storage methods (cryogenics, high pressure compression, and liquefaction techniques). These physical storage methods suffer from some drawbacks such as high cost and low storage efficiency [4,5].

The research for excellent hydrogen storage materials is always a topic of interest [4–6]. Recently, porous metal oxides (NiO, MgO and TiO_2) are studied for hydrogen storage [1–3,7–9]. Among others, TiO_2 possesses crucial advantages such as non-toxic and ecofriendly properties, which are exploited in several applications such as paints, fuel cell, solar cells, gas sensors, hydrogen storage, antibacterial materials, and photocatalysis [10]. There are materials which store hydrogen in the form of hydrides and materials which adsorb hydrogen molecules onto their surface [11,12]. Generally, hydrides function at high temperatures, while physisorbents require low temperatures to deliver sufficient sorption amounts of hydrogen. This is because the absorption enthalpies of chemical hydrides are normally high while adsorption enthalpies of physisorbents are normally low (e.g. 70 kJ mol^{-1} for MgH_2; and about 3–7 kJ mol^{-1} for carbon nanomaterials) [13,14]. Only materials functioning by the Kubas adsorption mechanism and the spillover effect would deliver substantial sorption capacities at temperature near ambient and at atmospheric condition without the necessity of using a heat-swing because these materials exhibit favored adsorption enthalpies [15,16]. Various polymorphs of TiO_2 are exploited as materials for Kubas-type hydrogen adsorption when the Ti^{4+} is partially reduced by various chemical agents [17]. The reduction process normally yields Ti^{3+}, and oxygen vacancies in the materials [18]. Ti^{3+} possesses d^1 electron configuration and it has been proved by several research groups that this Ti^{3+} can participate in a δ-π bonding motif with multiple dihydrogen molecules [19–22]. On the other hand, Ag nanoparticles have been employed as hydrogen adsorption materials because their capability of hydrogen sorption by spillover [23,24]. In this work, we exploit the chemically reduced TiO_2 as a hydrogen adsorption material and as a carrier to accommodate large quantities of Ag nanoparticles to enhance the sorption significantly by spillover mechanism. To the best of authors' best knowledge, this is the first report on mesoporous Ag/TiO_2 nanocomposite fabricated and applied for hydrogen storage studies.

Experimental procedure

Materials and methods

For the preparation of pure TiO_2 and nanocomposite Ag/TiO_2, the following chemicals were essential which were obtained from Sigma-Aldrich; silver acetate, titanium tetra isopropoxide (TTIP), citric acid, cetyltrimethyl ammonium bromide (CTAB) and isopropyl alcohol and entire aqueous solutions were prepared by double distilled water.

Preparation pure TiO_2 and TiO_2/Ag nanocoupled system

The sol-gel method was implemented for the preparation of pure TiO_2 material. In the beginning, 150 ml of is isopropyl alcohol solution was mixed with 30 ml of TTIP solution under vigorous stirring condition (600 rpm). Then, 0.5 mol of aqueous citrate solution (citric acid dispersed in deionized water) were added dropwise into the above solution. Subsequently, the colloidal gel solution was dried at room temperature for the materialization of TiO_2 pre-synthesized powder. At this stage, we differentiated the synthesis of pure TiO_2 and Ag/TiO_2 nanocomposite system. The pre-synthesized TiO_2 powder was calcined in a muffle furnace at 400 °C for 1 h and TiO_2 nanopowder was obtained. The preparation of the nanocomposite Ag/TiO_2 system adopted the thermal decomposition method reported previously [25,26]. In this work, we used as-synthesized TiO_2 powder and silver acetate (90:10 weight ratio) as raw materials. Then, the mixed raw materials were grounded for ~3 h using agate pestle and mortar. Afterwards, the grounded as synthesized mixed materials were calcined at 400 °C for 1 h to deliver nanocomposite Ag/TiO_2.

Characterization details

The XRD patterns of the synthesized materials were collected on an X-ray diffractometer (D5000 diffractometer, Siemens, USA) with $CuK_{\alpha 1}$ ($\lambda = 1.5406$ Å) radiation, structural information of synthetic materials were obtained by analysis of the XRD patterns. The morphological and internal structural remarks were examined via high resolution transmission electron microscopy (HR-TEM), selected area electron diffraction (SAED) and high-angle annular dark-field (HAADF) images using TEM, FEI TITAN G2 80-s300, operated at 300 KeV. The X-ray photoelectron spectroscopy (Thermo Scientific Escalab 250Xi) was used to find surface concentration and its oxidation states of the prepared materials. Nitrogen adsorption was conducted on a Micromeritics ASAP 2020 (USA) at 77 K. The pore size and pore volume were calculated by applying BET model on the nitrogen desorption data.

Measurements of hydrogen adsorption capacity of TiO_2/Ag nanocomposite

For evaluating the hydrogen adsorption of the prepared porous Ag/TiO_2 nanocomposite, the quartz-crystal microbalance (QCM) method was used [27,28]. Before the measurement, the sample was dispersed in isopropanol alcohol for sonication for 5 min. After that, the dispersed solution was deposited onto the top face of a quartz crystal (QC) and dried in air at room temperature. Then, the QC was placed on the head of the QCM system (from MDC model SQM-310). The above system was kept inside a stainless steel vacuum chamber. The temperature of the QC was maintained around 20 °C during the whole measurement process using water cooling. Afterwards, the inner atmosphere of the vacuum

chamber was evacuated with the help of rotatory and turbo pumps. Once, the chamber vacuum level was attained at 7×10^{-6} Torr, the vacuum gate valve was closed. Then, certain amounts of H_2 (Indura, 99.995%, O_2 < 5 ppm, H_2O < 8 ppm, CO_2 + CO < 4 ppm, N_2 < 20 ppm, and THC < 5 ppm) were injected in the chamber through a needle valve using different pressures between 3 and 100 Torr. The mass changes upon H_2 adsorption by the samples were determined by monitoring *in situ* changes of resonance frequency of QC during 7 min. After H_2 exposure, the chamber was evacuated and again the above step was repeated for increasing the exposure pressure value. From the monitored data, the resonance frequency versus time curve indicates the change of resonance frequency (Δf). The relationship between the mass added (Δm) to the QC due to H_2 adsorption and the shift in its resonance frequency (Δf) is represented by the Sauerbrey equation [27,28]:

$$\Delta f = -\frac{2f_0^2}{A\sqrt{\rho \cdot \mu}}\Delta m \quad (1)$$

where f_0 = resonance frequency of the fundamental mode (Hz), Δf = frequency change (Hz), Δm = mass change (g), A = effective area of the QC (cm^2), ρ = density of the QC (g/cm^3), and μ = bulk modulus for QC. The above equation specifies that the negative variation of the QC resonance frequency is dependent on the mass gain of the prepared samples upon H_2 adsorption ability. Further details of the Sauerbrey's equation and its description can be found from the previous reports [27,28].

Results and discussion

The structural confirmation of the synthesized materials is scrutinized via powder XRD technique and their resultant diffraction patterns are represented in Fig. 1. From the diffraction results, the pure TiO_2 material is well coordinated with tetragonal (JCPDS card no: 21-1272) anatase phase crystal structure. The lattice parameter of the pure TiO_2 is resulted at a = b = 3.789 ± 0.009 Å and c = 9.505 ± 0.012 Å, by Rietveld refinement. Furthermore, the prepared (via thermal decomposition method) Ag is screening, which shows face centered cubic crystal structure (JCPDS card no: 89-3722) with the lattice parameter value is a = 4.093 ± 0.011 Å. The crystallite size of the synthesized materials is intended by Scherrer formula and the values are presented in Table 1. The XRD result of the composite demonstrates that the incorporated Ag doesn't change the TiO_2 structure and vice versa. In this case, the formation of only metallic Ag is expected thanks to the use of CH_3COOAg. If other precursors, e.g. $AgNO_3$, is used, the decomposition products would contain mixed oxidation states of Ag, thus, an extra step is required to reduce them to pure metallic Ag.

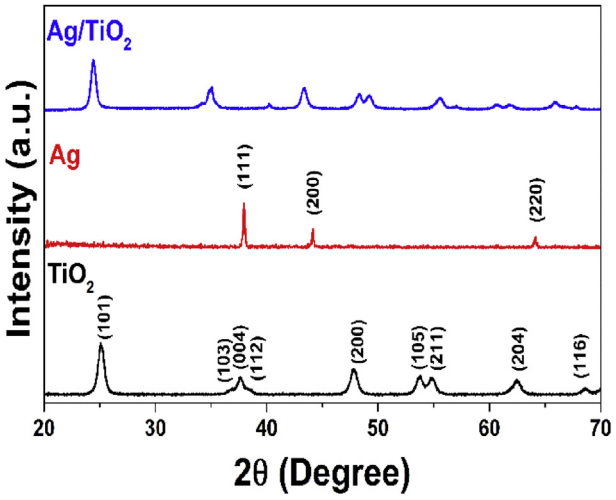

Fig. 1 – XRD pattern of the prepared materials.

The TEM, SAED, HR-TEM and HAADF images are exposed shape, size and structural evidence of the Ag/TiO_2 material. In Fig. 2a spectacles the TEM image of the synthesized Ag/TiO_2 materials and their outcome visibly epitomized that the tiny Ag nanoparticles are indiscriminately incorporated on the TiO_2 surface which symbolizes spherical in shape. The 4 nm–6 nm sized spherical small Ag particles were homogeneously decorating the larger 11 nm–13 nm sized TiO_2 particles (particle size distributions were shown in Fig. 1 SI).

The SAED image (Fig. 2b) of Ag/TiO_2 describes the d-space values alongside with their consistent hkl planes, which are denoted that cubic Ag beside with tetragonal TiO_2. The SAED outcomes are well accordance with XRD results.

On the other hand, for the close surveillance of the HR-TEM image (Fig. 2c) fascinatingly shows many line dislocation defects which are circulated in the image. Interim, the HAADF image (Fig. 2d) is reputed that the tiny Ag nanoparticles are scattered in the TiO_2 matrix. After the accumulation of Ag, the "pore or voids" are elevated in-between TiO_2 surface. During thermal decomposition, the condensation and nucleation progress lead to "pore or voids" in the Ag/TiO_2 materials [29]. Therefore, the morphological appearance of Ag/TiO_2 is signified that asymmetrical void space revolution and tiny Ag nanoparticles are incorporated into the TiO_2 materials.

The synthetic Ag/TiO_2 is studied by X-ray Photoelectron Spectroscopy (XPS). Fig. 3a shows the survey spectrum of the Ag/TiO_2 on which Ti, Ag, O, and C elements are detected. The HR-XP spectra of Ti 2p, Ag 3d, O 1s binding energies are corrected by using the C 1s peak (284.8 eV) as the standard. The HR-XP spectrum (Fig. 3b) of Ti 2p is attainable in the Ag/TiO_2 nanomaterials. This system has two prominent Ti 2p peaks which are responsible for the Ti 2p ½ and Ti 2p 3/2 (5.7 eV difference), which mostly represent Ti^{4+} state [30,31]. The existence of small quantities of Ti^{3+} species in the Ag/TiO_2 is

Table 1 – XRD crystallite size and textural information of prepared materials.

Samples	XRD crystallite size (D)- nm		Textural information		
	TiO_2	Ag	Pore volume BJH (cm^3/g)	Pore diameter BJH (nm)	Surface area BJH (m^2/g)
TiO_2	14.5	–	0.117	1.956	245.30
Ag/TiO_2	13.4	9.2	0.332	17.21	75.59

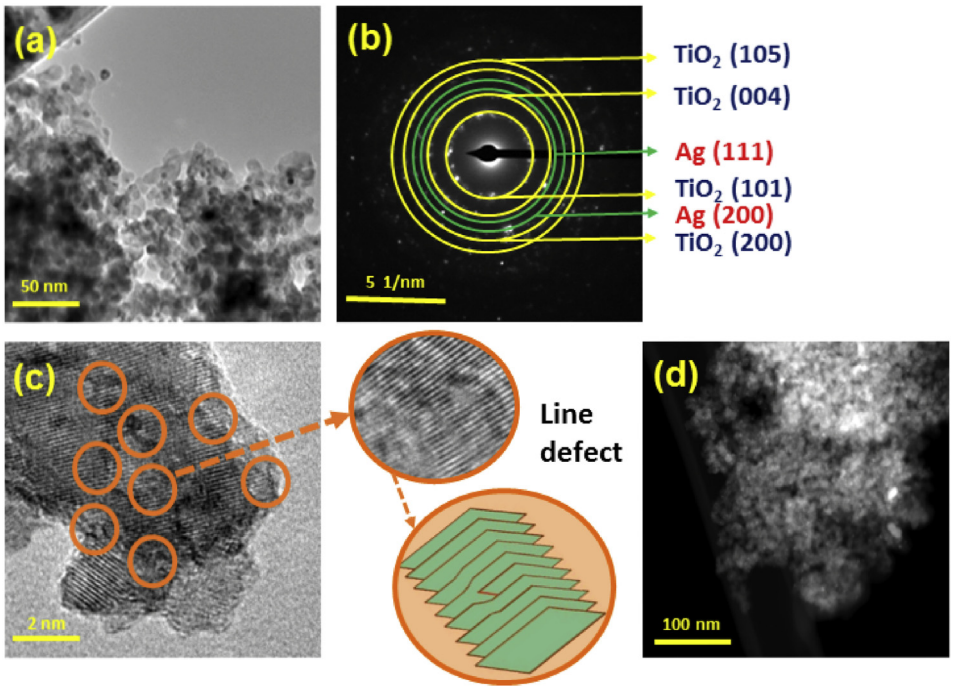

Fig. 2 – (a) TEM image of TiO_2/Ag (b) SAED pattern of TiO_2, (c) HR-TEM image of TiO_2/Ag and (d) HAADF image of TiO_2/Ag nanocomposite.

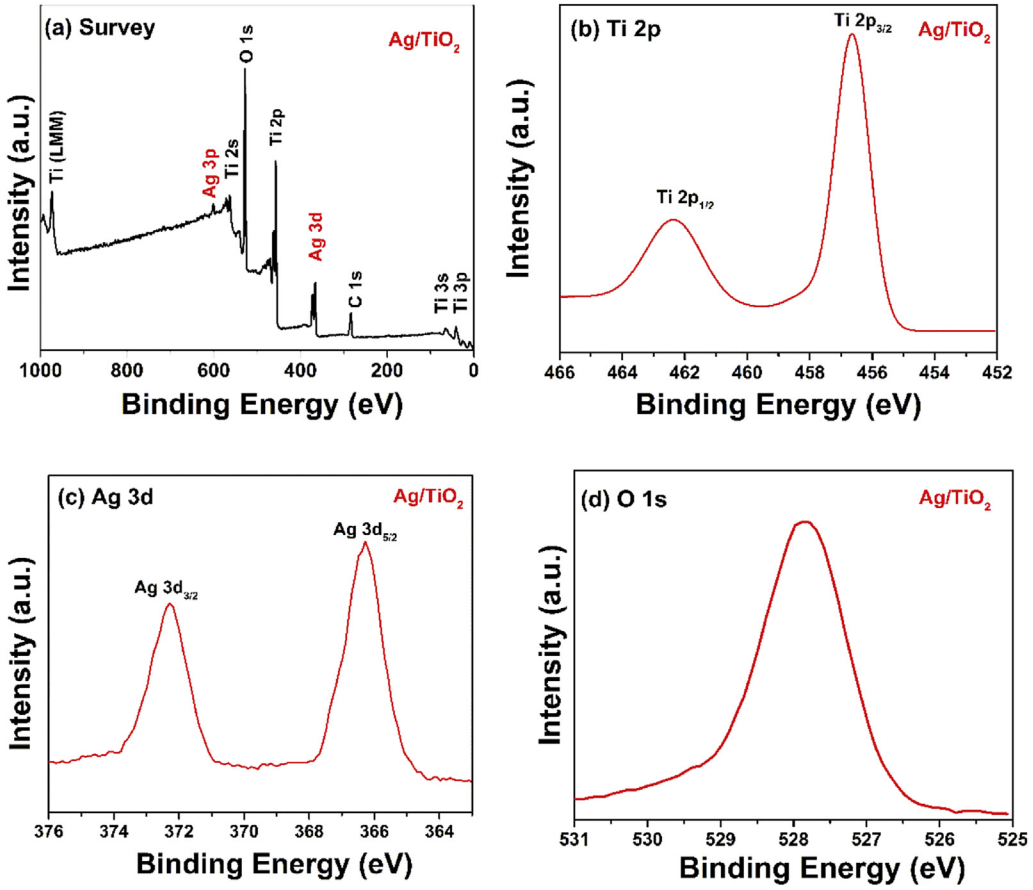

Fig. 3 – XP spectra of the Ag/TiO_2 material.

proved in the literature [32–34]. Compared with pure TiO_2 (Fig. 2, SI), the Ti 2p peaks of Ag/TiO_2 are shifted in lower binding energies. This reflection is due to the highly-dispersed silver nanoparticles or existing defects lead to formation Ti^{3+} state. This observation is reported in the literature [30,35,36]. However, accurate quantification of those Ti^{3+} species remains a challenge since they have low concentrations and are scattered within the materials [26].

The HR-XP spectrum of Ag 3d is demonstrated in Fig. 3c and their reliable binding energies are observed at 366.3 eV and 372.3 eV that postulates Ag $3d_{5/2}$ and Ag $3d_{3/2}$ peaks with the deviation of 6 eV [31]. This proves the existence of metallic silver in Ag/TiO_2 system, being agreed with XRD and HR-TEM results.

The textural information including porous volume, size, and specific surface area of the synthesized materials were evaluated by the BJH method and the values are denoted in Table 1. The pore distribution curves of TiO_2 and Ag/TiO_2 materials were shown in Fig. 4. The insets represent nitrogen (N_2) adsorption-desorption isotherms. The appearances of hysteresis loop of Ag/TiO_2 is exposed H3 type and it is entirely varied from pure TiO_2 system (which typically represents H4 type). This is due to nucleation and condensation process which lead to line defects, which creates "holes or big pores" on the Ag/TiO_2 surface [29].

Hydrogen storage by quartz crystal microbalance method

For the first time, the hydrogen adsorption behavior of Ag/TiO_2 nanocomposite is reported, even though some researchers have previously focused on theoretical studies [37]. The hydrogen storage capability of the prepared nanocomposite is measured using a quartz crystal microbalance based on QC resonance frequency change as a function of time when the sample is exposed to H_2 gas.

Fig. 5a and b depict the QC resonance frequency vs. time at different H_2 exposure pressures for TiO_2 and Ag/TiO_2 nanocomposite. We can obviously find out the different frequency shifts (Δf) depending on the exposure pressure for the calculation, the adsorbed hydrogen mass and determination of its storage capacity (wt. %) of the prepared nanocomposite, by using Saurbrey's equation (equation (1)). Fig. 5c represents the hydrogen adsorption behavior of the synthesized nanocomposite under different H_2 exposure pressures. The bare TiO_2 adsorbs about 0.251 wt% at 100.2 Torr, while the Ag/TiO_2 nanocomposite exhibits 0.917 wt% at 96.2 Torr under the same conditions. The presence of Ag nanoparticles enhances the adsorption capacity by 3.65 times. In this case, the effect of embedded noble metal nanoparticles is significant. Similarly, Sun et al. reported that hydrogen uptake capacity of mesoporous NiO is 0.08 wt% at 135 bar and the adsorption capacity is almost tripled after the addition of platinum metal into the mesoporous NiO, the Pt/NiO shows 0.22 wt% at 120 bar; this enhancement is attributed to the existence of metallic Pt clusters that change the electronic structure of NiO [38]. Hydrogen adsorption ability of the synthesized bare TiO_2 is superior (0.251 wt%) at low pressure (100.2 Torr) compared with previously reported data of TiO_2 and other metal oxides such as NiO and MgO [17,38]. The significant performance of bare TiO_2 could be attributed to its high surface area (245.3 m^2/g) and anatase phase purity, which are established by BET and XRD results. The adsorption power and thermodynamic stability of anatase phase is better than the rutile phase and this influences the hydrogen uptake capacity [39,40]. However, other publications reported higher hydrogen uptake performance [39–41]. This variation is due to morphology, surface area, pore size, and oxidation state of Ti [17,39,40]. Although, Hoang et al. clearly explained that the surface area alone is not the most important factor for hydrogen storage [17]. Moreover, the Ti^{4+} state (anatase or rutile) exhibits weaker Kubas interaction for hydrogen storage compared with the activity of Ti^{3+} [17,18,39].

Compared with the adsorption capacity of pristine TiO_2, the Ag/TiO_2 nanocomposite shows more than 3.65 times higher hydrogen storage capacity. Likewise, this nanocomposite exhibits better results compared with other hydrogen storage reports related with carbon nanotubes (CNT), metal covered with metal organic frame work (MOF), and MCM-41 [39,41–44]. The reason for the enhancement of hydrogen storage is as follows: the characterization results clearly specified that after the incorporation of metallic Ag on the surface of TiO_2, the electronic structure of TiO_2 is changed,

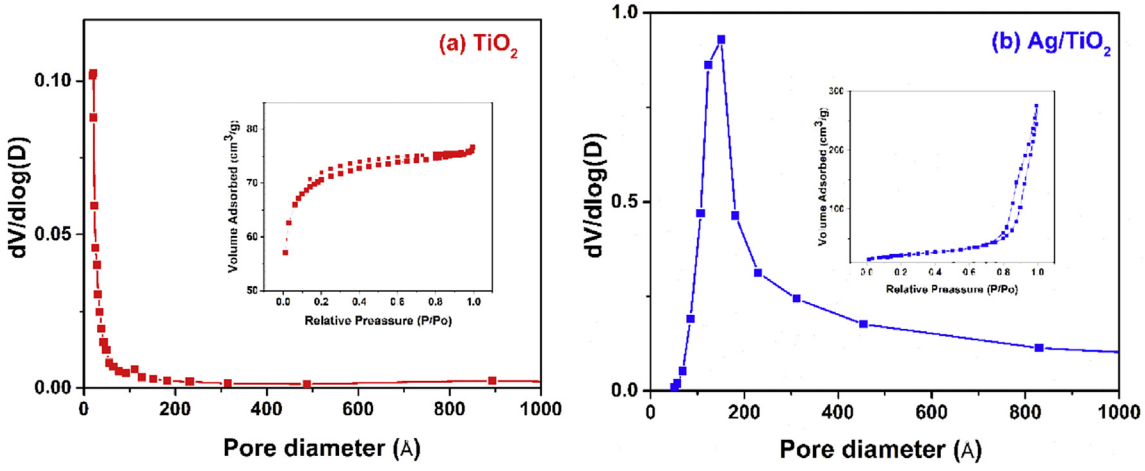

Fig. 4 – Pore distribution curves of (a) TiO_2 and (b) Ag/TiO_2 materials (inserted images represented nitrogen (N_2) adsorption-desorption isotherms).

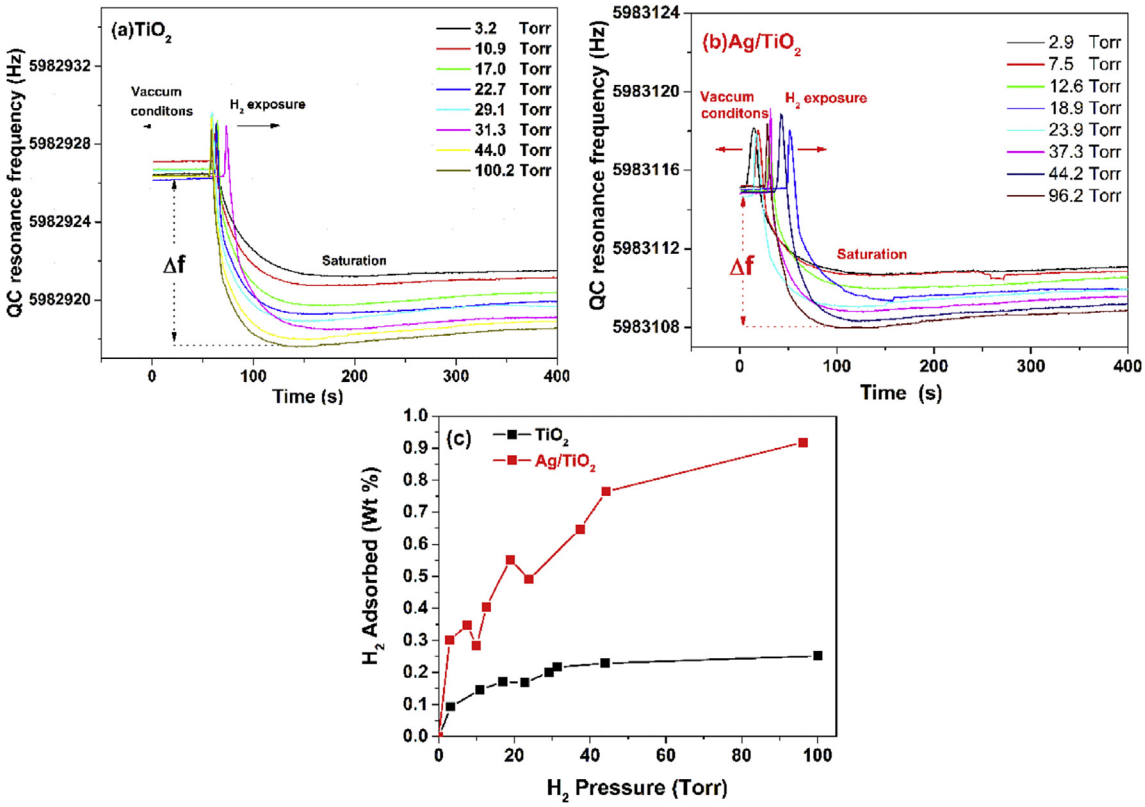

Fig. 5 – QC Resonance frequency as a function of time for (a) TiO_2, (b) Ag/TiO_2 nanocomposite, and (c) hydrogen adsorption behavior of the prepared TiO_2 and Ag/TiO_2 nanocomposite as a function of the H_2 exposure pressure.

the Ti^{4+} state is partially reduced to Ti^{3+} which is in agreement with the HR-TEM and XPS results. According to the 18-electron rule, up to five hydrogen molecules could be adsorbed by a single Ti^{3+} species [17,18]. Therefore, Ag/TiO_2 nanocomposite containing Ti^{3+} state is central for increasing hydrogen adsorption [17,18]. Moreover, a change in the oxidation state of titanium and the existence of metallic Ag makes strong interactions between hydrogen gas molecules with the Ag/TiO_2 materials. This interaction is potential for bonding of multiple hydrogen molecules with Ag/TiO_2 nanocomposite surface [17,18,45]. Furthermore, Ag nanoparticles are able to enhance hydrogen adsorption *via* spillover effect [23,46]. This may contribute significantly to the outstanding hydrogen adsorption of the Ag/TiO_2 nanocomposite. Previous studies reported that addition of Ag nanoparticles into carbon nanotubes increases the hydrogen sorption capacity by 40% (equivalent to a magnification of 1.4 times) at 298 K and 23 atm of H_2. After doping Ag on the TiO_2, we observe an enhancement of 3.65 times at a much lower testing pressure (96.2 Torr). This significant augmentation must be attributed to adsorption, Kubas binding of Ti^{3+} generated by linear defects, and spillover. The combination of Ag nanoparticles and the porous TiO_2 is very unique due to the reducibility of Ti^{4+} in the TiO_2 framework by Ag. Such a unique partnership is not observed on Ag-doped SiO_2 or Ag-doped carbon nanotubes because SiO_2 and carbon nanotubes are generally non-reducible materials. The optimization of Ag concentrations in the Ag/TiO_2 composite is necessary for constructing superior hydrogen storage material at low pressure and this is one of the tasks for our future work. Huizinga and Prins studied hydrogen adsorption on Pt/TiO_2 and proved that the spillover effect introduces the formation of H atoms, which could react with Ti^{4+} to create protons and Ti^{3+} [47,48]. Such a phenomenon may happen in Ag/TiO_2 nanocomposite, the H_2 molecules are dissociated into H atoms, which may react with Ti^{4+} to introduce more Ti^{3+} on the surface. The enrichment of Ti^{3+} concentration would accommodate even higher hydrogen adsorption capacity via Kubas binding mechanism. This means the very first absorbed H_2 molecules initiate a synergistic effect, which reversely enriches the concentration of Ti^{3+} and this Ti^{3+} is to provide more sorption centers for the newcomer hydrogen molecules.

Conclusion

The Ag/TiO_2 nanocomposite has been prepared characterized physically. Cubic Ag nanoparticles are scattered on the surface of the tetragonal anatase TiO_2 and partially reduce the TiO_2 carrier. As a result, Ti^{3+} is exist in the materials and the Ag/TiO_2 exhibit higher hydrogen adsorption capacity than the bare TiO_2 – up to 3.65 times. The outstanding enhancement may be due to the co-performance of Kubas-type hydrogen adsorption and spillover mechanism.

Acknowledgement

The authors (S.R. and F.G.) acknowledge the support of CONICYT through the project CONICYT/FONDAP/15110019.

Appendix A. Supplementary data

Supplementary data related to this article can be found at https://doi.org/10.1016/j.ijhydene.2017.12.080.

REFERENCES

[1] Chen S, Ostrom C, Chen A. Functionalization of TiO_2 nanotubes with palladium nanoparticles for hydrogen sorption and storage. Int J Hydrogen Energy 2013;38:14002–9.
[2] Bordbar M, Alimohammadi T, Khoshnevisan B, Khodadadi B, Faal AY. Preparation of MWCNT/TiO_2-Co nanocomposite electrode by electrophoretic deposition and electrochemical study of hydrogen storage. Int J Hydrogen Energy 2015;40:9613–20.
[3] Bajestani ZG, Akhlaghi O, Yurum Y, Yurum A. Synthesis of anatase TiO_2 with exposed (001) facets grown on N-doped reduced graphene oxide for enhanced hydrogen storage. Int J Hydrogen Energy 2017;42:6096–103.
[4] Felderhoff M, Weidenthaler C, Helmolt R, Eberle U. Hydrogen storage: the remaining scientific and technological challenges. Phys Chem Chem Phys 2007;9:2643–53.
[5] Reardon H, Hanlon JM, Hughes RW, Jopek AG, Mandal TK, Gregory DH. Emerging concepts in solid-state hydrogen storage: the role of nanomaterials design. Energy Environ Sci 2012;5:5951–79.
[6] Schlapbach L, Zuettel A. Hydrogen storage materials for mobile applications. Nature 2001;414:353–8.
[7] Gholami T, Niasari MS, Varshoy S. Electrochemical hydrogen storage capacity and optical properties of $NiAl_2O_4$/NiO nanocomposite synthesized by green method. Int J Hydrogen Energy 2017;42:5235–45.
[8] Yuan JG, Zhu YF, Li LQ, Wu Y, Zhou SX. Preparation and hydrogen storage property of Mg-based hydrogen storage composite embedded by polymethyl methacrylate. Int J Hydrogen Energy 2017;42:22366–72.
[9] Mortazavi SZ, Reyhani A, Mirershadi S. Hydrogen storage properties of multi-walled carbon nanotubes and carbon nano-onions grown on single and bi-catalysts including Fe, Mo, Co and Ni supported by MgO. Int J Hydrogen Energy 2017;42:24885–96.
[10] Ge M, Cao C, Huang J, Li S, Chen Z, Zhang KQ, et al. A review of one-dimensional TiO_2 nanostructured materials for environmental and energy applications. J Mater Chem A 2016;4:6772–801.
[11] Orimo SI, Nakamori Y, Eliseo JR, Zuettel A, Jensen C. Complex hydrides for hydrogen storage. Chem Rev 2007;107:4111–32.
[12] Rowsell JLC, Yaghi O. Strategies for hydrogen storage in metal-organic frameworks. Angew Chem Int Ed 2005;44:4670–9.
[13] Jia J, Sun CH, Shen SH, Zou J, Mao SS, Yao XD. Combination of nanosizing and interfacial effect: future perspective for designing Mg-based nanomaterials for hydrogen storage. Renew Sustain Energy Rev 2015;44:289–303.
[14] Xia YD, Yang ZX, Zhu YQ. Porous carbon-based materials for hydrogen storage: advancement and challenges. J Mater Chem A 2013;1:9365–81.
[15] Kubas GJ. Fundamentals of H_2 binding and reactivity on transition metals underlying hydrogenase function and H_2 production and storage. Chem Rev 2007;107:4152–205.
[16] Wang LF, Yang RT. New sorbents for hydrogen storage by hydrogen spillover-a review. Energy Environ Sci 2008;1:268–79.
[17] Hoang TKA, Antonelli DM. Exploiting the Kubas interaction in the design of hydrogen storage materials. Adv Mater 2009;21:1787–800.
[18] Hu X, Skadtchenko BO, Trudeau M, Antonelli DM. Hydrogen storage in chemically reducible mesoporous and microporous Ti oxides. J Am Chem Soc 2006;128:11740–1.
[19] Mason JA, Darago LE, Lukens Jr WW, Long JR. Synthesis and O_2 reactivity of a titanium(III) metal–organic framework. Inorg Chem 2015;54:10096–104.
[20] Simmons JM, Yildirim T, Hamaed A, Antonelli DM, Webb MI, Walsby CJ. Direct observation of activated hydrogen binding to a supported organometallic compound at room temperature. Chem Eur J 2012;18:4170–3.
[21] Hoang TKA, Morris L, Reed D, Book D, Trudeau ML, Antonelli DM. Observation of TiH_5 and TiH_7 in bulk-phase TiH_3 gels for Kubas-type hydrogen storage. Chem Mater 2013;25:4765–71.
[22] Hoang TKA, Morris L, Sun J, Trudeau ML, Antonelli DM. Titanium hydrazide gels for Kubas-type hydrogen storage. J Mater Chem A 2013;1:1947–51.
[23] Rather S, Naik M, Hwang SW, Kim AR, Nahm KS. Room temperature hydrogen uptake of carbon nanotubes promoted by silver metal catalyst. J Alloys Compds 2009;475:L17–21.
[24] Sun Y, Tao ZL, Chen J, Herricks T, Xia YN. Ag nanowires coated with Ag/Pd alloy sheaths and their use as substrates for reversible absorption and desorption of hydrogen. J Am Chem Soc 2004;126:5940–1.
[25] Pan ZW, Dai ZR, Wang ZL. Nanobelts of semiconducting oxides. Science 2001;291:1947–9.
[26] Saravanan R, Karthikeyan N, Gupta VK, Thirumal E, Thangadurai P, Narayanan V, et al. ZnO/Ag nanocomposite: an efficient catalyst for degradation studies of textile effluents under visible light. Mater Sci Eng C 2013;33:2235–44.
[27] Far RE, Diaz-Droguett DE, Rojas S, Avila JI, Romero CP, Lievens P, et al. Quantitative determination of hydrogen absorption by Pd cluster-assembled films using a quartz crystal microbalance. Thin Solid Films 2012;522:199–203.
[28] Kulchytskyy I, Kocanda MG, Xu T. Direct mass determination of hydrogen uptake using a quartz crystal microbalance. Appl Phys Lett 2007;91:113507 (1–3).
[29] Navarro CR, Agudo ER, Luque A, Navarro ABR, Huertas MO. Thermal decomposition of calcite: mechanisms of formation and textural evolution of CaO nanocrystals. Am Mineral 2009;94:578–93.
[30] Khan MM, Ansari SA, Pradhan D, Ansari MO, Han DH, Lee J. Band gap engineered TiO_2 nanoparticles for visible light induced photoelectrochemical and photocatalytic studies. J Mater Chem A 2014;2:637–44.
[31] Khan MM, Ansari SA, Amal MI, Lee J, Cho MH. Highly visible light active Ag@TiO_2 nanocomposites synthesized using an electrochemically active biofilm: a novel biogenic approach. Nanoscale 2013;5:4427–35.
[32] Fu Y, Du H, Zhang S, Huang W. XPS characterization of surface and interfacial structure of sputtered TiNi films on Si substrate. Mater Sci Eng 2005;403:25–31.
[33] Atuchin VV, Kesler VG, Pervukhina NV, Zhang Z. Ti 2p and O 1s core levels and chemical bonding in titanium-bearing oxides. J Electron Spectrosc Relat Phenom 2006;152:18–24.

[34] Kakavandi R, Savu S-A, Caneschi A, Chasse T, Casu MB. At the interface between organic radicals and TiO_2(110) single crystals: electronic structure and paramagnetic character. Chem Commun 2013;49:10103–5.
[35] Sivaranjani K, Gopinath CS. Porosity driven photocatalytic activity of wormhole mesoporous $TiO_{2-x}N_x$ in direct sunlight. J Mater Chem 2011;21:2639–47.
[36] Wang S, Qian H, Hu Y, Dai W, Zhong Y, Chen J, et al. Facile one-pot synthesis of uniform TiO_2–Ag hybrid hollow spheres with enhanced photocatalytic activity. Dalton Trans 2013;42:1122–8.
[37] Pillay D, Wang Y, Hwang GS. A comparative theoretical study of Au, Ag and Cu adsorption on TiO_2 (110) rutile surfaces. Kor J Chem Eng 2004;21:537–47.
[38] Sun X, Hwang JY, Shi S. Hydrogen storage in mesoporous metal oxides with catalyst and external electric field. J Phys Colloid Chem 2010;114:7178–84.
[39] Rather SU. Hydrogen storage of nanostructured TiO_2-impregnated carbon nanotubes. Int J Hydrogen Energy 2009;34:961–6.
[40] Zhongyi Z, Huimiao C, Ning W, Yujun C. Hydrogen storage property of porous/hollow TiO_2 using yeast as template. Rare Metal Mater Eng 2013;42:2467–71.
[41] Guo ZP, Yuan L, Konstantinov K, Huang ZG, Liu HK. Preparation of spherical clusters of metal oxide nanorods and their hydrogen storage behavior. Mater Lett 2006;60:3891–4.
[42] Ramachandran S, Ha JH, Kim DK. Hydrogen storage characteristics of metal oxide doped Al–MCM-41 mesoporous materials. Catal Commun 2007;8:1934–8.
[43] Li G, Kobayashi H, Taylor JM, Ikeda R, Kubota Y, Kato K, et al. Hydrogen storage in Pd nanocrystals covered with a metal–organic framework. Nat Mater 2014;13:802–6.
[44] Morel M, Mosquera E, Droguett DED, Carvajal N, Roble M, Rojas V, et al. Mineral magnetite as precursor in the synthesis of multi-walled carbon nanotubes and their capabilities of hydrogen adsorption. Int J Hydrogen Energy 2015;40:15540–8.
[45] Wang P, Wang AM, Zhang HF, Ding BZ, Hu ZQ. Hydrogenation characteristics of Mg-TiO_2 (rutile) composite. J Alloys Compds 2000;313:218–23.
[46] Hohmeyer J, Kondratenko EV, Bron M, Kröhnert J, Jentoft FC, Schlögl R, et al. Activation of dihydrogen on supported and unsupported silver catalysts. J Catal 2010;269:5–14.
[47] Huizinga T, Prins R. Behavior of titanium(3+) centers in the low- and high-temperature reduction of platinum/titanium dioxide, studied by ESR. J Phys Chem 1981;85:2156–8.
[48] Prins R. Hydrogen spillover. facts and fiction. Chem Rev 2012;112:2714–38.